Electronic structure of Mn-doped ZnO by x-ray emission and absorption spectroscopy

2008 J. Phys.: Condens. Matter 20 275205

(http://iopscience.iop.org/0953-8984/20/27/275205)

IOP Publishing Journal of Physics: Condensed Matter

J. Phys.: Condens. Matter **20** (2008) 275205 (7pp) doi:10.1088/0953-8984/20/27/275205

Electronic structure of Mn-doped ZnO by x-ray emission and absorption spectroscopy

F Bondino[1], K B Garg[2], E Magnano[1], E Carleschi[1,3], M Heinonen[4], R K Singhal[2], S K Gaur[2] and F Parmigiani[1,3]

[1] Laboratorio Nazionale TASC INFM-CNR, Basovizza-Trieste, Italy
[2] Department of Physics, University of Rajasthan, Jaipur-302004, India
[3] Dipartimento di Fisica, Università degli Studi di Trieste, Trieste, Italy
[4] Department of Material Science, Turku University, Turku-20014, Finland

E-mail: bondino@tasc.infm.it

Received 13 February 2008, in final form 14 April 2008
Published 2 June 2008
Online at stacks.iop.org/JPhysCM/20/275205

Abstract

We report an investigation of Mn-doped ZnO pellets with diluted Mn concentration by soft-x-ray emission and absorption spectroscopy. We have compared the electronic structure of two samples with different Mn concentration and different magnetic properties at room temperature: ferromagnetism in one case ($Zn_{0.98}Mn_{0.02}O$) and no magnetic order in the other ($Zn_{0.96}Mn_{0.04}O$). The results show that most of the Mn ions of the ferromagnetic sample are in the divalent state. For the nonmagnetic sample, a larger contribution of higher oxidation Mn states is present, which can be correlated to the suppressed ferromagnetism. The presence of oxygen atoms bonded to Mn ions and hybridized Mn 3d–O 2p states has been detected in both compounds. The partial density of states in the valence band has been measured with x-ray emission spectroscopy and the Mn 3d states have been found inside the bandgap of ZnO

(Some figures in this article are in colour only in the electronic version)

1. Introduction

The discovery that wide-band-gap ZnO doped with diluted transition metals can show ferromagnetism above room temperature has attracted considerable interest due to the potential technological applications in devices wherein the ferromagnetism would exist together with the semiconducting, optical, and piezoelectric properties of ZnO. Ferromagnetism above room temperature in diluted Mn-doped ZnO was first reported for a sample with less than 4% Mn concentration [1]. The origin of ferromagnetism in diluted magnetic semiconductors (DMS) such as transition-metal-doped ZnO has been long debated, but it is yet to be resolved. An extrinsic origin of ferromagnetism, such as metal cluster formation, should be considered for each sample [2]. Even if Mn clusters are expected to give an antiferromagnetic rather than a ferromagnetic order, very small clusters can be ferromagnetic [3]. Various mechanisms giving rise to ferromagnetism have been suggested. In ZnO DMS ferromagnetism is theoretically foreseen by the mediation of shallow donors or acceptors [4] or by the holes in the valence band [5]. It has also been suggested [6] that the room-temperature ferromagnetism in the Mn–Zn–O system is associated with the coexistence of Mn^{3+} and Mn^{4+} via a double-exchange mechanism. Recent x-ray-magnetic-circular dichroism (XMCD) measurements show that for diluted $Zn_{1-x}Co_xO$ films, Co ions substituted for Zn in the ZnO matrix are not directly at the origin of ferromagnetism [2, 7, 8] and that the anion sublattice may instead be responsible for the ferromagnetism [8].

In this work we have attempted to shed light on this problem by comparing the electronic structure of two Mn-doped ZnO samples showing different magnetic properties at 300 K. Our aim is to find out how the changes in the electronic structure can be correlated to the observed magnetic properties. Most of the x-ray spectroscopic investigations performed so far on diluted metal-doped ZnO have focused on thin films, prepared mostly by pulsed-laser ablation [2, 9–15] or other deposition methods [16] and, in a few cases, on powders [17].

Here we have investigated two polycrystalline Mn–ZnO pellets doped with diluted (2% and 4%) Mn concentration. The samples were characterized by a superconducting quantum interference device (SQUID) and x-ray diffraction (XRD) [18]. These characterization measurements established that the compounds have the ZnO lattice and no detectable impurities. In particular, for $Zn_{0.98}Mn_{0.02}O$ XRD with Rietveld analysis showed that the sample is single phase. Magnetization versus temperature measurements have been made on both the samples from 20 to 350 K. However, measurements beyond this range on either side were not possible. $Zn_{0.98}Mn_{0.02}O$ displays clear ferromagnetic patterns and magnetic ordering throughout the range, while $Zn_{0.96}Mn_{0.04}O$ shows no ordering down to 20 K. The magnetic moment of the 2% sample increases by almost a factor of 2 going from 300 K (0.000 08 emu) to 20 K (0.000 15 emu). The presence of mixed phases in the samples is unlikely since no signatures of multiple transition temperatures were seen in the SQUID measurements [18].

In this work, the electronic structure of these two samples is investigated employing Mn L_{23}, O K and Zn L_{23} x-ray absorption spectroscopy (XAS), Mn L$\alpha\beta$, O Kα and Zn L$\alpha\beta$ x-ray emission spectroscopy (XES) and resonant XES (RXES) at the O K edge. In particular, our aim is to measure the element- and orbital-resolved density of states around the Fermi level, to obtain indications about the Mn oxidation state and coordination and to compare the Mn L$\alpha\beta$ XES and O K edge RXES of the two Mn–ZnO samples with different magnetic properties.

2. Experiment

The measurements were performed on $Zn_{0.98}Mn_{0.02}O$ and $Zn_{0.96}Mn_{0.04}O$ pellets (hereafter referred to as the 2% sample and 4% sample, respectively) and on some reference samples, i.e. MnO, Mn metal, $La_{1.2}Sr_{1.65}Ca_{0.15}Mn_2O_7$ bilayer manganite and an intermetallic MnSi sample[5], all scraped in UHV before each measurement. The nominal bulk Mn concentration of the two samples (2% and 4%) was verified during the same experiment by comparing the intensity ratio of the O K and Mn Lα in the normal XES spectra of the two Mn-doped ZnO samples and MnO.

The measurements were performed at the BACH beamline of Elettra in Trieste [19]. The measurements were performed at room temperature at a pressure of $<5 \times 10^{-10}$ mbar.

The XES spectra were acquired with a grating fluorescence spectrometer [20]. The acquisition time for the XES data varied from a few minutes for O K and Zn Lα XES to several hours for the Mn L$\alpha\beta$ XES from the diluted Mn–ZnO samples, due to the combined effect of the low Mn concentration in the samples and the low efficiency of the XES process.

The O K XAS were detected in total fluorescence yield (FY) by a photodiode detector placed at 30° from the normal-incident photon beam with a resolution of 0.27 eV at 530 eV. The FY mode was chosen for O K XAS due to the deeper sampling sensitivity of this detection mode with respect to electron yield. For a qualitative interpretation of the XAS lineshape as the absorption coefficient of the excited atom, the saturation spectral distortions are not significant at normal incidence for the O K-edge [21]. The combination of low Mn concentration and low efficiency of the fluorescence process at the Mn L_{23}-edge or possible other effects prevented us from obtaining the Mn L_{23} XAS in FY from the diluted Mn–ZnO samples. Mn L_{23} XAS was obtained, with a shorter probing depth (∼15–20 Å), in the total electron yield (TEY) by means of a current amplifier with a resolution of 0.4 eV.

The data were corrected for the energy-dependent incident photon flux. The incident photon energy was calibrated by measuring Au $4f_{7/2}$ photoelectron core level with a 150 mm-VSW analyzer. O K and Mn Lα emission energies were calibrated using the elastic peaks in the XES spectra.

3. Results and discussion

The Mn L_{23} XAS measured in TEY from the 2% sample is reported in figure 1(a). This spectrum is compared to the Mn L_{23} XAS obtained during the same beam-time under the same experimental conditions from MnO (Mn^{2+} reference system), Mn metal and the $La_{1.2}Sr_{1.65}Ca_{0.15}Mn_2O_7$ bilayer manganite (reference system for a mixed valent compound, theoretically 40% Mn^{4+}/60% Mn^{3+}).

It is well known that the position and the lineshape of the L_3-edge shift and change significantly when the charge state and crystal field of Mn change. The Mn L_{23} XAS of the 2% sample is quite different from the Mn L_{23} XAS of the bilayer manganite, which has the main peak centered at 2.5 eV higher photon energy with respect to the main peak of the 2% sample (at 640 eV). The Mn L_{23} XAS of the 2% sample is also different from the XAS spectrum of Mn metal, which does not display multiplet structures. This excludes the possibility that Mn impurities are all segregated in metallic clusters. Instead, the Mn L_{23} XAS from the 2% sample shows multiplet structures qualitatively similar to those of MnO, suggesting that Mn ions in Mn–ZnO are nearly divalent. However, a closer look at the Mn L_3-edge (figure 1(b)) reveals several differences between the two spectra. Firstly, the lower energy multiplet lines at 639 eV do not appear for $Zn_{0.98}Mn_{0.02}O$. Secondly, there is an increased spectral weight around 642 eV in $Zn_{0.98}Mn_{0.02}O$. These differences indicate that the local environments of Mn in $Zn_{0.98}Mn_{0.02}O$ and MnO are different. The absence of the multiplet lines at 639 eV can be assigned to a lower absolute value of the crystal field parameter $10D_q$ for $Zn_{0.98}Mn_{0.02}O$ with respect to the corresponding value for MnO. Multiplet calculations show that by reducing the absolute value of $10D_q$, not only the intensity of the multiplet lines at 639 eV is reduced, but also the intensity of the lines at 642 eV is increased at the same time [22]. As an example of such variation, we report in figure 1(a) two XAS multiplet calculations performed for Mn^{2+} ($3d^5$) in sites with O_h point symmetry with the cubic crystal field $10D_q = 0.8$ eV for MnO [23] and with the same parameters of [8] used for Co in Co-doped ZnO (C_{3v} point symmetry, $10D_q = -0.47$, $D_\sigma = 0.06$ eV, and $D_\tau = -0.03$ eV), assuming that Mn substitutes

[5] The MnSi sample was kindly provided by Dr Fabrizio Carbone and professor Dirk van der Marel.

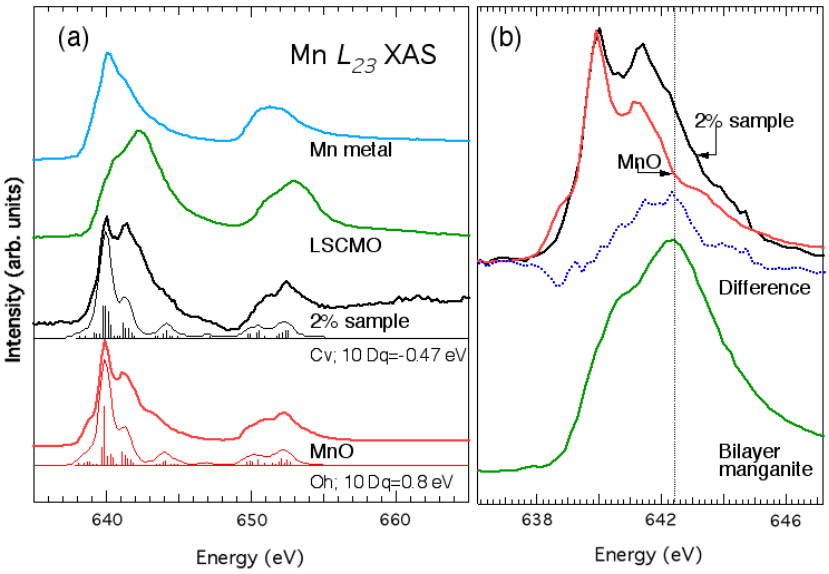

Figure 1. (a) From top to bottom: Mn L_{23} XAS spectra, measured under the same experimental conditions (TEY, $T = 300$ K, normal photon incidence) of Mn metal, $La_{1.2}Sr_{1.65}Ca_{0.15}Mn_2O_7$ bilayer manganite (LSCMO), $Zn_{0.98}Mn_{0.02}O$, calculated XAS for Mn^{2+} in C_{3v} symmetry with $10D_q = -0.47$, $D_\sigma = 0.06$ eV, and $D_\tau = -0.03$ eV, MnO and calculated XAS for Mn^{2+} in O_h symmetry with $10D_q = 0.8$ eV. (b) Top spectra: Mn L_3 XAS of the $Zn_{0.98}Mn_{0.02}O$ compared to Mn L_3 XAS of MnO; bottom spectra: difference spectrum between the Mn L_3 XAS of MnO and the Mn L_3 XAS of $Zn_{0.98}Mn_{0.02}O$ compared to Mn L_3 XAS of $La_{1.2}Sr_{1.65}Ca_{0.15}Mn_2O_7$ bilayer manganite.

for Zn, for the 2% sample[6] [24]. However, the agreement between experiment and calculation is not ideal and the variation of the spectral weight around 642 eV is more difficult to rationalize since it can also be determined by the presence of Mn sites with higher oxidation states, most likely Mn^{3+}/Mn^{4+}. Since a weighted sum of the spectra calculated for different valencies has the disadvantage of depending on too many parameters (weighting factors, crystal field parameters, etc), a qualitative indication of the changes between the Mn–ZnO and MnO may perhaps be directly obtained from their Mn L_3 XAS spectra. The Mn L_3 XAS difference spectrum between the Mn–ZnO and MnO spectra, which is reported in figure 1(b), indeed shows similarities with the main Mn L_3 XAS peak of the bilayer manganite. Furthermore, we also notice that the Mn L_3 XAS spectrum of the 2% sample is also similar to the spectra of $Zn_{0.97}Mn_{0.03}O$ films reported in [16], where the doping dependence indicated that the Mn L_{23} XAS contained an increasing signature of higher charge states for increasing Mn concentration.

In figure 2 we have plotted on the same energy scale O K XAS, O Kα, Zn Lα, and Mn Lα emissions (the intensities have been normalized arbitrarily) from the 2% and 4% samples. The O K XAS of the 2% sample is similar to the 3% Mn-doped thin films in [16]. O K XAS measured in FY can be regarded as a reliable measurement of the empty oxygen p bulk partial density of states [21]. With respect to the O K XAS of undoped ZnO [12, 25], both the 2% and the 4% samples show a small extra spectral weight in the pre-edge region, around 528.5 eV. The presence of this extra spectral weight, which is higher for the 4% sample (see inset of figure 2), was also previously detected in TEY O K XAS of Mn-doped ZnO [16] and in Co-doped ZnO [15, 17]. Although for the latter system, lattice defects had been suggested as a possible origin of this extra spectral weight [15]. A similar pre-threshold peak usually appears in systems, such as manganites and cuprates, when there is hybridization between transition-metal 3d states with O 2p orbitals. Similarly, in these systems also, the pre-threshold peak can be assigned to the O 2p holes created after hybridization with Mn 3d states. Given the bulk sensitivity of the FY measurement, the observation of this peak for concentrations as low as 2% (where the system is ferromagnetic) would mean that Mn atoms have significant interaction with O atoms in the bulk too.

O K XES spectra of the 2% and 4% samples reported in figure 2 were measured at an excitation energy of 534.5 eV and with a combined incident/emission energy resolution of 0.6 eV. The O K XES spectra are plotted on the same energy scale (top scale) as the corresponding O K XAS curves, using the elastic peak as the calibration point. The O K XES spectra measured at this energy have normal fluorescence character since no significant changes in the energy position and relative intensity of the emission structures appear for higher excitation energies. At the same time, the excitation energy used for these O K XES spectra is low enough so that no spurious high-energy shake-up satellites are produced [26]. Due to dipole selection rules, the O K x-ray emission is produced during the transition of 2p electrons of the valence band to the 1s core hole. The O K XES spectra measured at an excitation energy lower than the threshold for the double excitation can be considered as an experimental probe of oxygen p partial density of states, with negligible core–hole effects, as discussed in detail by Anisimov *et al* [27]. The O K emission spectrum thus reflects the O 2p occupied states, while O K XAS reflects the O p unoccupied states. A bandgap of about 2.6 eV and 2.7 eV is observed between the valence and conduction O 2p states in the 2%

[6] The calculations have been performed with the program Missing 1.1 by Riccardo Gusmeroli based on Cowan's Hartree–Fock atomic code.

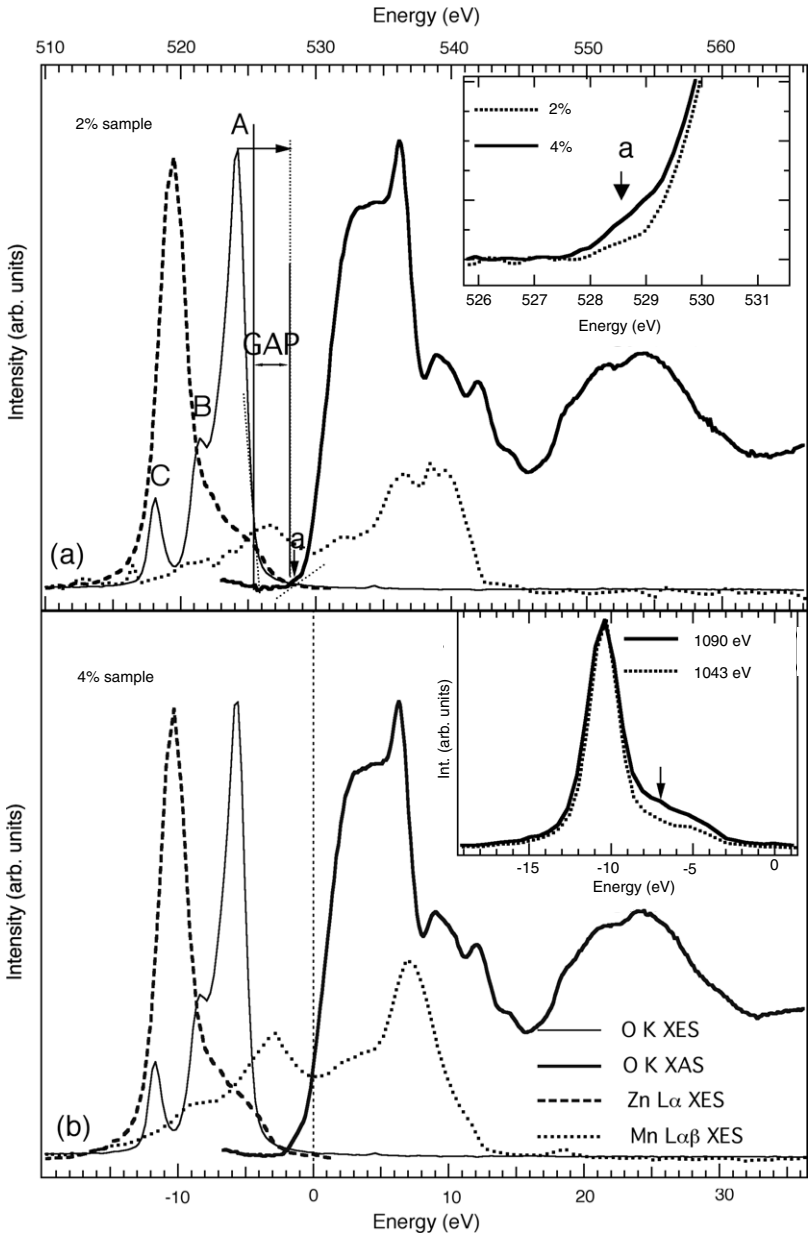

Figure 2. (a) O K XES, Zn Lα XES, Mn Lα XES, and O K XAS of the 2% Mn-doped sample plotted on the same energy scale. Inset: O K XAS pre-threshold region of the 2% and 4% samples. The pre-peak *a* is indicated by an arrow. (b) O K XES, Zn Lα XES, Mn Lα XES and O K XAS of the 4% Mn-doped sample plotted on the same energy scale. The intensities are normalized arbitrarily. The top scale represents the emission and incident photon energy for the XES and XAS spectra, respectively; the bottom scale represents a binding-energy scale as described in the text. Inset: Zn Lα XES spectra acquired at two different excitation energies, 1043 eV and 1090 eV, which are at ∼21 eV and 68 eV above the Zn L_3 threshold, respectively.

and 4% samples, respectively. This value is lower than the bandgap estimated with the same method for undoped ZnO (3.3 eV) [25]. The reduced bandgap in the present case may be associated with the presence of Mn 3d orbitals which generate some extra 2p holes at the anion sites appearing in the pre-threshold O K XAS.

The Zn Lα and Mn Lα emission spectra reported in figure 2 were measured with excitation energy of 1090.0 eV and 650.6 eV respectively. O K XAS/XES and Mn Lα XES have been aligned on the same scale (bottom scale) by subtracting the O 1s binding energy of 529.8 eV and the Mn 2p binding energy of 640.5 eV, respectively, measured from 5% Mn:ZnO [28]. The Zn Lα emission energy was calibrated to the value 1011.7 eV reported in [29] since it was not possible to detect the elastic peak for this excitation energy. The binding-energy scale (bottom scale) was then obtained by subtracting the binding energy of Zn $2p_{3/2}$ (1022.1 eV) reported in [30] for 1.3% Cu-doped[7] ZnO [31, 32].

[7] The resulting Zn Lα peak position in the valence band scale carries the uncertainty of the calibration of the Lα emission line (ranging from 1011.7 to 1012 eV for different compounds) [29] and the Zn $2p_{3/2}$ binding energy (ranging from 1021.2 to 1022.5 eV) [31]. However, using this calibration, the Zn Lα peak maximum is found at −10.4 eV, which is close to the value of −10.7 eV reported in the literature for the Zn 3d binding energy in the Mn/ZnO(0001) system [32].

The Lα line is created during the transition of 3d and 4s electrons from the valence band to the $2p_{3/2}$ core hole. The 4s states, however, do not generally make a significant contribution to the Lα XES, despite being involved in dipole allowed transitions [33]. If one neglects core–hole effects and the intensity redistribution produced by dipole matrix elements, Zn Lα and Mn Lα emissions are mainly related to Zn 3d and Mn 3d partial DOS. Hence, the XES spectra should in principle reflect the site-specific partial densities of states of the different elements in the compound.

However, as for the O K XES spectra [26], it is important to single out the possible spurious satellites in Zn and Mn L$\alpha\beta$ XES spectra. These satellites can be avoided by exciting the system near the absorption threshold. Indeed, spurious satellites in the Zn L$\alpha\beta$ XES spectra were observed in Zn metal at excitation energies already below the L_2 threshold, but the satellites become less pronounced and eventually disappear on approaching the L_3 threshold [34]. The Zn Lα XES spectra of the 2% and 4% samples acquired at 1090 eV appear to be composed of a main line at a binding energy of 10.4 eV and a high-energy emission broad structure, located at 3–8 eV above the main peak (figure 2). In the inset of figure 2(b), the Zn Lα XES acquired at a lower excitation energy, 1043 eV, which is ∼21 eV above the Zn L_3 threshold, is compared to the spectrum obtained at 1090 eV, which is about 68 eV above the Zn L_3 threshold. At the lowest excitation energy the high-energy structures are strongly suppressed. Therefore, these high-energy structures appear to be strongly affected by spurious satellites generated by spectator vacancies. In the absence of Zn L$\alpha\beta$ XES acquired with lower excitation energy and neglecting the possible effects of a core–hole initial state, only the main peak at 10.4 eV can be associated to Zn 3d partial density of states.

The Mn L$\alpha\beta$ XES shown in figure 2 was measured with excitation energy set on the L_2 threshold, ∼10 eV above the Mn L_3 threshold. During the same experiment, the Mn Lα XES spectra were also measured at lower excitation energies, e.g. on and 5 eV above the L_3 threshold (not shown), which are low enough that high-energy satellites cannot be produced. The comparison between these spectra indicates that the Mn L$\alpha\beta$ XES spectra in figure 2 do not display detectable satellites, but only fluorescence structures at constant emission energy, corresponding to a binding energy of ∼3 eV and ∼7–10 eV.

We notice that the first peak in the Mn L$\alpha\beta$ XES spectra at ∼3 eV appears inside the bandgap of ZnO. The presence of a high-energy peak at about 7–10 eV in Mn Lα XES is emphasized by the excitation energy on the L_2 resonance (650.6 eV). This Mn emission peak overlaps with O K x-ray emission structures, indicating significant hybridization between Mn 3d and O 2p states. Furthermore, we notice that this peak appears at the L_2 resonance also in other oxides, such as MnO and the bilayer manganite, while it is absent in intermetallic Mn compounds such as MnSi and Mn_4Si_7 [35], supporting the assignment of this peak to O 2p–Mn 3d hybridized states.

In order to check the possible effects of many-body correlation and core–hole initial state in the interpretation of the

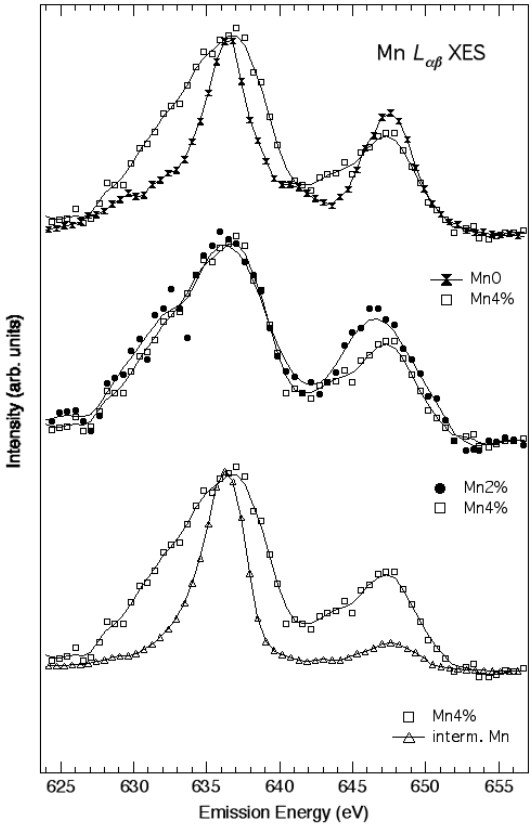

Figure 3. Mn L$\alpha\beta$ XES of the 2% and 4% samples, compared to MnO and intermetallic Mn (MnSi) measured in the same experimental geometry at 300 K for excitation energy well above the L_2 absorption edge. The markers are the experimental points; the lines are guides to the eyes.

XES spectra as partial density of states, we compare the experimental Zn Lα, Mn Lα and O K XES to the theoretical electronic structures of ZnO-based dilute magnetic semiconductors calculated within the self-interaction-corrected local density approximation reported in [36]. For (Zn, Mn)O, the calculations found the top of the valence band composed by Mn 3d states at about 2–3 eV below the Fermi level, then a second structure of overlapping Mn 3d and O 2p states between 3 and 7 eV, and a structure due to Zn 3d states centered at ∼10.5 eV. Thus, the results of the calculations match well with the results obtained from XES experimental data.

The normal emission O K and the Zn Lα-edge XES spectra of the 2% and 4% samples do not show detectable differences either in intensity or in the lineshape. A clear difference between the two samples is found instead in the branching ratio, BR, of Mn $I(\mathrm{L}\beta)/I(\mathrm{L}\alpha)$ XES. In figure 3 we show the normal XES spectra from the two samples measured at excitation energies of 664 eV. In the same figure we report the Mn L$\alpha\beta$ XES spectra of MnO and an intermetallic Mn compound (MnSi), measured in the same experimental geometry. All spectra have been normalized to the Lα emission peak. At normal emission for excitation energies well above the Mn L_{23}-edge, the BR is 0.6 for the 2% sample, while it is 0.5 for the 4% sample. For Mn oxides, the $I(\mathrm{L}\beta)/I(\mathrm{L}\alpha)$ XES BR decreases with the increasing covalency of Mn

ions. If compared to MnO whose BR $I(\mathrm{L}\beta)/I(\mathrm{L}\alpha) = 0.6$ (measured under the same experimental conditions and without self-absorption corrections), the BR of the Mn-doped ZnO samples is similar, while it is much higher with respect to intermetallic samples such as MnSi, Mn_4Si_7 [35], or metallic Mn (BR < 0.2). The BR therefore supports the mainly divalent MnO-like environment for Mn interstitials in the lower doped sample. However, we observe that the BR decreases going from the 2% Mn-doped ZnO to the 4% doped sample. The BR of the 4% doped sample is lower than that of MnO. Since increasing oxidation state leads to reduction of the $I(\mathrm{L}\beta)/I(\mathrm{L}\alpha)$ XES ratio, an increased number of Mn ions with higher oxidation state may be present in the 4% Mn-doped sample besides the majority divalent ions. The data, therefore, show that the $I(\mathrm{L}\beta)/I(\mathrm{L}\alpha)$ XES ratio is suppressed going from the magnetic 2% sample to the nonmagnetic 4% sample. This result is consistent with a similar decrease of the BR from a magnetic to nonmagnetic Mn-doped ZnO thin film with the same 2% Mn concentration [14]. This general behavior can be correlated to the possible formation of a secondary phase, where Mn is in a higher oxidation state, which can be correlated to the suppressed ferromagnetism. This behavior appears to contradict the Mn^{3+}/Mn^{4+} double-exchange mechanism suggested to explain the ferromagnetism.

The resonant x-ray emission spectra across the O K-edge of the two samples are shown in figure 4. For energies above 533.4 eV, for both the samples three clear emission structures at 524.2 eV, 521.2 eV, and 517.9 eV, labeled A, B, and C respectively, appear at constant emission energy. These three normal fluorescence structures are identical for the two samples and they are also very similar to those observed in undoped ZnO [25].

Instead, at lower excitation energies, in particular when the incident photon energy is tuned on the O K pre-edge peak, the O K RXES spectra display a strong dependence on the excitation energy and a difference in the intensity between the two samples. At excitation energy tuned on the pre-edge (527.9 eV), for both samples there is only a broad structure peaked at ∼523.8 eV with a low emission energy shoulder and a very weak structure at 517.9 eV. By monotonically increasing the excitation energy, the peak at 523.8 eV shifts gradually to higher energy. When plotting the spectra on an energy loss scale with the elastic peaks set at 0 eV (see inset of figure 4, which reports the first three spectra of the 4% sample), this peak (labeled as R2) appears at a constant energy loss of ∼4.4 eV for excitation energies tuned on the pre-edge threshold (527.9–528.6 eV). By following the vertical line in the main panel of figure 4 as a guide to the eye, we observe that the R2 peak, after the gradual shift to higher emission energies with increasing incident energy, at a slightly higher excitation energy (spectra 5 and 6 in figure 4) shifts back by 0.25 to 524.2 eV and then remains at constant emission energy for still higher energies. This backshift at increasing excitation energy is unexpected, but it was already observed in O K RXES of undoped ZnO nanoparticles [25], where it was attributed to the selective resonant enhancement of a different kind of O site. Also for the Mn–ZnO samples, this peak may correspond to an O site with different coordination and, in this

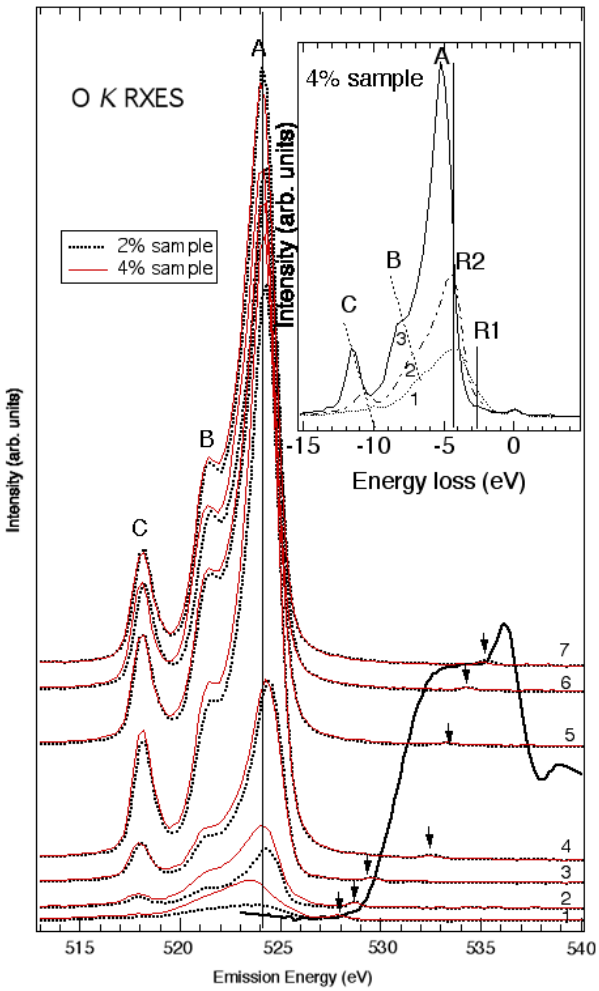

Figure 4. O K RXES spectra of the 2% and 4% samples measured at the excitation energies across the O K absorption edge. The excitation energies are indicated by the arrows on the elastic peaks (which are weak, but still visible). The O K XAS of one sample (2%) is reported in the same figure (thick curve). The inset shows the first three spectra of the 4% sample. A, B, and C indicate the normal fluorescence peaks, while R1 and R2 the scattering structures discussed in the manuscript.

case, it is likely to be associated to the O sites bonded to Mn atoms. Interestingly, while the O K RXES spectra of the two samples do not display any significant difference, neither in the shape nor in the intensity, and are practically identical for any excitation energy above 533.4 eV, significant differences are observed in the intensity of the O K RXES spectra of the two samples for excitation energies below 533.4 eV, with the emission intensity of the 4% sample always higher than the 2% sample, with the spectral lineshape remaining the same. In particular, the emission intensity for the 4% sample is twice as high as that for the 2% sample at 527.9 eV on the pre-threshold peak, where the main structure has constant energy loss. The possibility that the R2 structure is associated to a low-energy transition involving O atoms bonded to Mn is consistent with the increased spectral intensity at higher Mn doping level.

In the RXES spectra 1 and 2 excited on the pre-threshold XAS at 527.9 and 528.6 eV respectively, for both samples there is also another shoulder that appears at an energy loss

around 2.5–3 eV (labeled as R1 in the inset of figure 4). This shoulder is detectable in a very narrow energy range corresponding to the O K pre-peak and it is very weak probably because it may be related to the Mn 3d states. It is not possible to draw definite conclusions, but it is interesting that cluster model calculations [37] and optical and electron absorption spectroscopy measurements have found the signature of transition in $Zn_{1-x}Mn_xO$ around the same energy (3 eV) and assigned it to metal-to-ligand conduction band charge-transfer [4, 38] or to d–d transition [37]. It is interesting to notice that also the RXES measurements at Mn L_3 resonance from the 2% and 4% samples (not reported here) show the presence of two well-defined structures, one around 7.6 eV and the other at 3 eV from the elastic peak, the latter being at the same energy loss found for R1 in the O K RXES. However, the low incident energy resolution which was necessary for the Mn L_3 RXES, due to the very diluted Mn concentration, prevented our establishing whether these structures disperse with the excitation energy following a Raman-like behavior and can thus be identified as RIXS structures.

4. Conclusions

The electronic structure of two Mn-doped ZnO pellets with different magnetic properties at room temperature has been determined by a combined absorption and emission spectroscopy experiment.

The electronic structure of Mn–ZnO as probed by x-ray emission spectroscopy (XES) reveals that Mn 3d states have a component located inside the bandgap of ZnO and another component overlapping with the O 2p states. A signature of hybridization between O 2p holes and Mn 3d states is also found in O K XAS.

The multiplet structure in the Mn L_{32} absorption and the branching ratio in the Mn L$\alpha\beta$ emission reveal that Mn has mainly a divalent ionic configuration in the ferromagnetic sample with 2% Mn concentration, while there is also an indication of the presence of higher Mn oxidation states in the nonmagnetic sample with 4% Mn concentration.

Acknowledgments

We acknowledge Dr F Carbone and Professor D van der Marel for the MnSi sample. We also thank R Gusmeroli for the freeware distribution of the Missing 1.1 code for multiplet calculations. KBG, RKS, and SKG also acknowledge UGC (project No. F.10-12/2004(SR)), DST (travel), and Elettra (local) support.

References

[1] Sharma P, Gupta A, Rao K V, Owens F J, Sharma R, Ahuja R, Guillen J M O, Johansson B and Gehring G A 2003 *Nat. Mater.* **2** 673–7
[2] Rode K, Mattana R, Anane A, Cros V, Jacquet E, Contour J-P, Petroff F and Fert A 2008 *Appl. Phys. Lett.* **92** 012509
[3] Bobadova-Parvanova P, Jackson K A, Srinivas S and Horoi M 2005 *J. Chem. Phys.* **122** 014310
[4] Kittilstved K R, Norberg N S and Gamelin D R 2005 *Phys. Rev. Lett.* **94** 147209
[5] Dietl T, Ohno H, Matsukura F, Cibert J and Ferrand D 2000 *Science* **287** 1019
[6] García M A *et al* 2005 *Phys. Rev. Lett.* **94** 217206
[7] Gacic M, Jakob G, Herbort C, Adrian H, Tietze T, Brueck S and Goering E 2007 *Phys. Rev.* B **75** 205206
[8] Barla A *et al* 2007 *Phys. Rev.* B **76** 125201
[9] Keavney D J, Buchholz D B, Ma Q and Chang R P H 2007 *Appl. Phys. Lett.* **91** 012501
[10] Okabayashi J *et al* 2004 *J. Appl. Phys.* **95** 3573
[11] Kobayashi M *et al* 2005 *Phys. Rev.* B **72** 201201(R)
[12] Guo J-H *et al* 2007 *J. Phys.: Condens. Matter* **19** 172202
[13] Ishida Y *et al* 2007 *Appl. Phys. Lett.* **90** 022510
[14] Chang G S, Kurmaev E Z, Jung S W, Kim H-J, Yi G-C, Lee S-I, Yablonskikh M V, Pedersen T M, Moewes A and Finkelstein L D 2007 *J. Phys.: Condens. Matter* **19** 276210
[15] Krishnamurthy S *et al* 2006 *J. Appl. Phys.* **99** 08M111
[16] Thakur P, Chae K H, Kim J-Y, Subramanian M, Jayavel R and Asokan K 2007 *Appl. Phys. Lett.* **91** 162503
[17] Chang G S, Kurmaev E Z, Boukhvalov D W, Finkelstein L D, Colis S, Pedersen T M, Moewes A and Dinia A 2007 *Phys. Rev.* B **75** 195215
[18] Garg K B *et al* 2007 unpublished
[19] Zangrando M, Finazzi M, Paolucci G, Comelli G, Diviacco B, Walker R P, Cocco D and Parmigiani F 2001 *Rev. Sci. Instrum.* **72** 1313
[20] Cocco D, Zangrando M, Matteucci M, Bondino F, Platè M, Zacchigna M, Parmigiani F, Nelles B and Prince K C 2004 *AIP Conf. Proc.* **705** 873
[21] Krol A *et al* 1990 *Phys. Rev.* B **50** 8257
Carboni R, Giovannini S, Antonioli G and Boscherini F 2005 *Phys. Scr.* T **155** 986
[22] van der Laan G and Kirkman I W 1992 *J. Phys.: Condens. Matter* **4** 4189
[23] de Groot F M F 1991 *PhD Thesis* University of Nijmegen
[24] Cowan R D 1981 *The Theory of Atomic Structure and Spectra* (Berkley: University of California Press)
[25] Dong C L, Persson C, Vayssieres L, Augustsson A, Schmitt T, Mattesini M, Ahuja R, Chang C L and Guo J-H 2004 *Phys. Rev.* B **70** 195325
[26] Kennard E H and Ramberg E 1934 *Phys. Rev.* **46** 1040
[27] Anisimov V I, Kuiper P and Nordgren J 1994 *Phys. Rev.* B **50** 8257
[28] Chen W, Wang J and Wang M-r 2007 *Vacuum* **81** 894
[29] Lawniczak-Jablonska K, Kachniarz J and Spolnik Z M 1999 *J. Alloys Compounds* **286** 71
[30] Herng T S, Lau S P, Yu S F, Yang H Y, Tengand K S and Chen J S 2007 *J. Phys.: Condens. Matter* **19** 236214
[31] Wagner C D, Naumkin A V, Kraut-Vass A, Allison J W, Powell C J and Rumble J R *NIST Standard Reference Database 20* (Version 3.4 (Web Version) http://srdata.nist.gov/xps/)
[32] Guziewicz E, Kopalko K, Sadowski J, Guziewicz M, Golacki Z, Kanski J and Ilver L 2005 *Phys. Scr.* T **115** 541
[33] Pederson M R, Liu A Y, Baruah T, Kurmaev E Z, Moewes A, Chiuzbaian S, Neumann M, Kmety C R, Stevenson K L and Ederer D 2002 *Phys. Rev.* B **66** 014446
[34] Wassdahl N, Rubensson J-E, Bray G, Glans P, Bleckert P, Nyholm R, Cramm S, Mårtensson N and Nordgren J 1990 *Phys. Rev. Lett.* **64** 2807
[35] Bondino F *et al* 2007 unpublished
[36] Toyoda M, Akai H, Sato K and Katayama-Yoshida H 2006 *Physica* B **376/377** 647
[37] Mizokawa T, Nambu T, Fujimori A, Fukumura T and Kawasaki M 2002 *Phys. Rev.* B **65** 085209
[38] Fukumura T, Jin Z, Ohtomo A, Koinuma H and Kawasaki M 1999 *Appl. Phys. Lett.* **75** 3366